INTERNATIONAL SCIENTIFIC AND VOCATIONAL JOURNAL (ISVOS JOURNAL)

Vol.: 9 Issue: 1 Date: 30.06.2025 Received: 22.05.2025 Accepted: 13.06.2025 Final Version: 25.06.2025

ISVOS Journal, 2025, 9(1): 145-160 – DOI: 10.47897/bilmes.1704235

A Multidimensional Investigation from Electronic Properties to Biological Activity of 2-[(4-Hydroxyphenyl)iminomethyl]thiophene by DFT, HOMO-LUMO, MEP, NLO, NBO, Mulliken, Hirshfeld and Molecular Docking Analyses

Cem Cüneyt Ersanlı [a,1], Sultan Başak [b]

[a] Sinop University, Faculty of Arts and Science, Department of Physics, Sinop, Türkiye
ORCID ID: 0000-0002-8113-5091
[b] Sinop University, Institue of Postgrade Education, Department of Chemistry, Sinop, Türkiye
ORCID ID: 0000-0003-0541-3667

Abstract

Ever since they were first discovered, Schiff bases have been the subject of much attention due to their functional chemical character and intensive interdisciplinary applications, particularly in medicinal chemistry. The compounds are gaining interest due to their ability to provide stable coordination complexes and exhibit a vast array of biological activities, such as antimicrobial, anticancer, and antiviral activities. In this contribution, the structure of 2-[(4-hydroxyphenyl)iminomethyl]thiophene, (**I**), a compound previously described in the literature, was ascertained with great accuracy employing up-to-date quantum chemical calculations to better understand its electronic behavior and reactivity. In addition, the antiviral, anticancer, and anti-Alzheimer activity of the compound was thoroughly investigated employing a battery of in vitro and computational assays. The results proved the active character of the compound against various biological targets, and that it was a multiradial drug candidate. Furthermore, ADME-Tox properties were examined to evaluate the pharmacokinetic profile and toxicity of the compound. Favorable ADME properties and a low likelihood of toxicity highlight the molecule's suitability for continued development. The research showed the chemical stability of the molecule, its high hyperconjugation and strong intramolecular stability as factors contributing to its overall strength. These structural features also hold out promise for drug development since they can lead to increased efficacy and long-lasting activity in biological systems. Furthermore, molecular docking simulations corroborated the efficacy of the compound as a potential ligand that could interact with key biological macromolecules, rendering it a highly effective ligand with high binding affinity. This also contributes to its potential as a lead compound for new therapeutic drugs. Lastly, this research not only describes the structure and properties of (**I**), but also provides a pragmatic window through its pharmacological potential, worthy of experimental and clinical studies to explore fully its promise in drug discovery.

Keywords: "Computational quantum methods, Hirshfeld surface characterization, molecular docking, ADME properties, toxicity analysis."

1. Introduction

Hugo Schiff, a German chemist, was the first to synthesize Schiff bases by condensing primary amines with aldehydes or ketones, utilizing the azeotropic distillation method [1]. Schiff bases have a general formula represented as $R_1R_2C{=}NR_3$, where R1 and R2 groups can be alkyl, aryl, or heterocyclic groups with various substituents. In Schiff base synthesis, the nucleophilic nitrogen of the primary amine attacks the electrophilic carbon of the carbonyl with the generation of a hemiaminal intermediate. The dehydration of the intermediate yields an imine compound [2]. In the initial step of this general reaction mechanism, the aldehyde or ketone reacts with the primary amine to yield a tetrahedral intermediate known as a carbinolamine. This intermediate undergoes acid- or base-catalyzed dehydration. Upon isolation of the product or removal of water, the reaction completes. The stability of Schiff bases may vary depending upon the nature of the aryl or alkyl substituents. Aryl-substituted Schiff bases are more stable than alkyl-substituted ones [3]. Moreover, Schiff bases derived from aromatic aldehydes are more stable than those derived from aliphatic aldehydes due to the possibility of extensive conjugation. Schiff bases derived from ketones are more stable than those derived from aldehydes due to reduced steric hindrance. The ease of synthesis, structural versatility, and strong electrophilic character of Schiff bases have generated interest in their research and their investigation using interdisciplinary approaches [2]. These properties have made Schiff bases omnipresent ligands in coordination chemistry [4]. Apart from these inherent reasons, Schiff bases also possess high reactivity, strong biological activity [5], and remarkable versatility [6], which further increase their significance. These properties have not only intensified active research on Schiff bases but also promoted

[1] Corresponding Author
E-mail Address: ccersanli@sinop.edu.tr

the advancement of coordination chemistry [7]. Schiff bases have thus assumed an interdisciplinary role and have attracted a great deal of interest among researchers for applications as optical chemical sensors [8], as efficient catalysts [9], and as anti-Alzheimer [10,11], anticancer [12-14], antibacterial [15-17], and antiviral [18-21] agents.

As per World Health Organization (WHO), cancer is a heterogeneous group of disorders characterized by the unregulated proliferation of abnormal cells, capable of initiating in virtually any tissue. These cells often infiltrate adjacent structures and may disseminate to distant organs through metastasis. On a global scale, cancer constitutes a major health concern and is the second foremost cause of death [22]. Unlike normal cells, cancer cells not only possess the ability to grow infinitely but also other hallmark features like the ability to evade apoptosis, to induce angiogenesis, and the ability to escape cell cycle checkpoints that under normal circumstances regulate cell advancement. This sequential process of change is called oncogenesis and can be caused by both genetics and the environment [23]. For the human body to maintain homeostasis, all physiological processes must function flawlessly. Any deviation caused by genetic mutation or environmental stress could result in numerous states of disease. For instance, receptor tyrosine kinases (RTKs), coded for by approximately two-thirds of the human genome's tyrosine kinase genes, play a crucial role in cellular signaling [24]. Exposed on the cell membrane, RTKs bind to particular ligands and convey external signals into the cell to initiate an intracellular cascade reaction. The signaling cascades are vital in sustaining homeostasis and controlling fundamental life processes. Some RTKs are required for normal cellular physiology. Genetic or environmental changes might, however, interfere with these proteins to cause disease, including malignancy [25]. c-KIT or CD117 is a family of proto-oncogene RTKs that encode the c-KIT receptor. It was initially identified in 1986 as the cellular homolog of the viral oncogene v-KIT found in the Hardy-Zuckerman 4 feline sarcoma virus [26]. c-KIT must bind to its specific ligand, stem cell factor (SCF), to be activated [27]. c-KIT is a transmembrane receptor protein consisting of an extracellular domain responsible for ligand binding, a single transmembrane segment, and intracellular domains with tyrosine kinase activity [28]. c-KIT is present in several types of cells throughout the body. Upon binding to SCF, c-KIT becomes activated, and the downstream signaling pathways are induced that regulate important processes such as proliferation, survival, and migration-functions essential for the maintenance of physiological homeostasis [29]. However, gain-of-function mutations in c-KIT can lead to constitutive activation of c-KIT without SCF binding. This SCF-independent activation can disrupt the normal regulatory signaling pathways and cause loss of homeostasis [30]. They have been linked with a variety of different cancers, some of which include certain types of melanoma [31], gastrointestinal stromal tumors (GISTs), acute myeloid leukemia (AML) [32], and seminomas.

Ebolaviruses (EBOV) are negative-sense RNA *Filoviridae* family viruses. The viruses are mostly transmitted through direct contact with body fluids or through close contact with the bodies of infected patients. EBOV infections have been noted to cause deadly disease with high mortality rates [33]. The 2013-2016 West African outbreak underscored Ebolavirus's high epidemic potential, with more than 28.000 cases and around 11,000 deaths reported [34,35]. The virus was originally named after the Ebola River, near where it was first identified. EBOV primarily targets the immune system, resulting in a sudden reduction in lymphocyte counts. This immune suppression typically results in disseminated intravascular coagulation (DIC) that is accountable for multi-organ failure [36]. The incubation period of the disease ranges from 2 to 21 days, and the onset of symptoms is extremely similar to the flu. In the progressive evolution of the disease, vomiting, diarrhea, and liver and kidney damage are observed [37]. Drugs approved for the treatment of EBOV include monoclonal antibodies. However, the cost of these treatments and their cold chain shipping requirements greatly limit access, particularly to impoverished communities [38]. Therefore, small-molecule drugs that can act against specific phases of the viral life cycle are a more effective and affordable treatment option [39].

Neurodegenerative diseases are characterized by the gradual and progressive loss of specific neuronal populations within distinct regions of the central nervous system. These disorders represent a major cause of mortality in industrialized nations, especially among the elderly [40]. Although each of these ailments has unique symptoms and pathophysiology, they share much in common with respect to the causative factors [10]. One of the most popular neurodegenerative diseases is Alzheimer's disease (AD) that was first described in 1901 by Dr. Alois Alzheimer in his report of a patient's symptoms [41]. According to global statistics, AD has most frequently been linked to elderly individuals, with an estimated 5 million new cases every year. Estimated statistics reveal that by the year 2050, one in every 85 individuals globally could have AD [42]. AD is associated with memory loss, inability to form new memory, neurotransmitter imbalances, and irreversible damage of cholinergic neurons, all of which affect the neuron communication [43]. Despite the many theories that have arisen regarding the etiology of AD, one of the most compelling contenders is the cholinergic hypothesis [44]. This postulates that a fall in the concentration of acetylcholine (ACh) has the potential to trigger cognitive dysfunctions and also lead to the onset of neurodegenerative diseases. ACh is metabolized by the enzyme acetylcholinesterase (AChE), which thus has the primary task of determining the concentration of accessible ACh in the synaptic cleft [10]. ACh is found in most of the central nervous system, including the brain, where it lives as a fundamental neurotransmitter. Decreased ACh synthesis and increased neural hydrolysis retard neural transmission [45]. Therefore, a balance within this process is seen as essential to the regulation of the progression of neurodegenerative conditions. Advances in technology and research are enabling new inhibitors targeted to and regulating these processes to be developed [46,47].

In this study, the physical and chemical properties of the Schiff base compound 2-[(4-hydroxyphenyl)iminomethyl]thiophene, (**I**), whose structure was previously elucidated experimentally by X-ray diffraction by Kazak et al. [48], were investigated using quantum chemical calculations. In addition, the anticancer, antiviral and anti-Alzheimer activities of the compound were modeled using molecular docking methods and the ADME-Tox properties were further elucidated. Special emphasis is placed on

its interaction with proteins associated with Alzheimer's disease and Ebola virus, due to their urgent clinical significance and the structural compatibility of Schiff bases with key molecular targets involved in these pathologies. AD is a progressive neurodegenerative disorder linked to reduced acetylcholine levels, where AChE inhibitors are primary therapeutic agents [49]. Schiff bases with aromatic and heterocyclic groups have demonstrated potent AChE inhibition in several prior studies [50.51], motivating their further investigation. Similarly, EBOV, a member of the Filoviridae family, causes severe hemorrhagic fever with high mortality. The development of small molecules targeting key viral proteins is essential, particularly due to the high cost and storage limitations of existing monoclonal antibody therapies [52]. Recent research highlights Schiff bases as effective scaffolds for the design of viral enzyme inhibitors [53]. Thus, exploring compound **I**'s binding affinity with Ebola-related proteins represents a logical and timely extension of Schiff base-based antiviral drug discovery.

2. Materials and Method

In current theoretical research, physical, chemical, and biological aspects of the (**I**) molecule [48] were studied. The research included Hirshfeld surface analysis, frontier molecular orbital (HOMO-LUMO) analysis, molecular electrostatic potential (MEP) mapping, nonlinear optical (NLO) properties, natural bond orbital (NBO) analysis, Mulliken charge distribution, and prospective antiviral, anticancer, and anti-Alzheimer activity of the compound. All the theoretical calculations were carried out using the density functional theory (DFT) method in the Gaussian 03 package [54]. The B3LYP hybrid functional [55], which is based on Becke's exchange functional [56] and the Lee-Yang-Parr correlation functional [57], was employed in conjunction with the 6-311++G(d,p) basis set [58]. The molecule's structure was optimized in the gas phase, and the results were visualized using the GaussView 4.1.2 program [59]. To examine intermolecular interactions and packing in crystals, the CrystalExplorer 17.5 software [60] was utilized. Hirshfeld surfaces [61-63] and two-dimensional fingerprint plots [62] were generated with the compound's crystallographic input file (CIF). Protein structures of c-KIT, Ebola glycoprotein, and acetylcholinesterase for the biological tests were downloaded from the Protein Data Bank [Ebola virus glycoprotein PDB ID: 4IBB [64], c-KIT PDB ID: 4U0I [65], and acetylcholinesterase PDB ID: 1QTI [66]. Docking studies utilized AutoDock Vina 1.5.6 [67], and the resulting interactions were visualized with Biovia software [68]. Pharmacokinetic and toxicological features (ADME-Tox) of the compound were predicted using the SwissADME platform [69].

3. Results and discussion

3.1. Optimized Molecular Structure

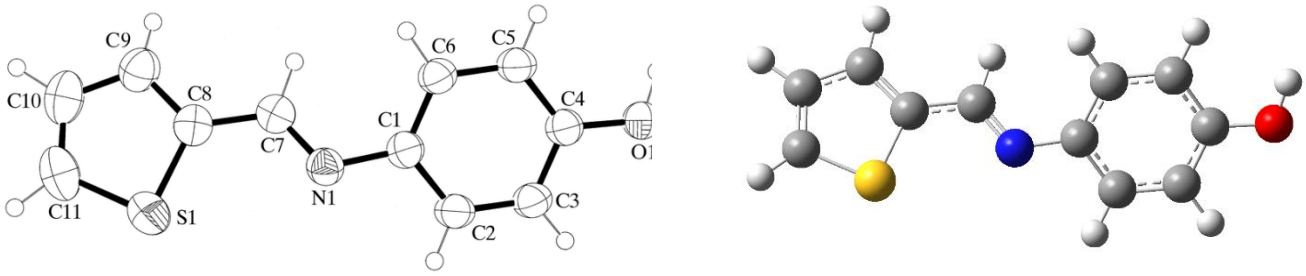

(a) **(b)**

Fig. 1. (a) ORTEP-III representation of the crystal structure of (I) (b) representation of the optimized molecular structure.

The optimized structure of the title compound is Fig. 1. The compound has a thiophene ring and a benzene ring, with interplanar angle calculated as 35.51º. It has been found that Schiff bases exhibit two different tautomeric forms: the keto-amine and enol-imine tautomers [10]. There are some ways in which a tautomeric form adopted by a molecule can be identified, one of which is geometrical analysis. By examining specific bond lengths and taking into account double bond character, the primary tautomeric structure can be inferred. The existence of a comparatively short C=N bond indicates the enol-imine structure. Table 1 contains bond lengths, bond angles, and torsional angles in the title compound, while Fig. 1 represents the molecular structure that was achieved after geometry optimization. From the inspection of Fig. 1 and Table 1, it is found that the C7–N1 bond possesses significant double bond character with a calculated bond length of 1.280 Å and experimental bond length of 1.282 (2) Å. The shortish C–N bond provides proof of the existence of a C=N double bond, confirming the enol-imine tautomer. For the O1–C4 bond, a bond lengthes of theoretical 1.370 and experimental 1.358 (2) Å were seen Table 1. This comparatively long C–O bond, combined with the abbreviated C=N bond, once again predominates in the enol-imine tautomeric form of the molecule. Inspection of the literature shows that the equivalent structures with the enol-imine tautomeric form also have normal bond lengths [70-73].

Table 1. X-ray diffraction method and DFT/B3LYP/6-311++G(d,p) calculated selected geometric parameter values (Å, °).

Bond Length and Bond Angles	Experimental	Theoretical
S1-C11	1.705 (3)	1.730
S1-C8	1.712 (2)	1.750
O1-C4	1.358 (2)	1.370
N1-C7	1.282 (2)	1.280
N1-C1	1.422 (2)	1.403
C7-C8	1.447 (3)	1.445
C8-C9	1.369 (3)	1.380
C9-C10	1.400 (3)	1.420
C10-C11	1.336 (4)	1.369
C7-N1-C1	119.69 (16)	120.85
N1-C7-C8	123.52 (18)	122.64
C6-C1-N1	124.37 (16)	124.07
O1-C4-C5	123.21 (16)	122.73
O1-C4-C3	117.72 (16)	117.59
C9-C8-S1	110.36 (16)	110.90
C10-C11-S1	112.41 (19)	112.39

3.2. Frontier Molecular Orbitals (FMOs)

FMOs play important roles in understanding the chemical reactivity, stability, and electronic characteristics of a molecule. FMOs are mostly studied at two levels, i.e., highest occupied molecular orbital (HOMO) and lowest unoccupied molecular orbital (LUMO). The HOMO is the most energetic orbital to donate an electron, while the LUMO is the lowest energy orbital to accept an electron [74,75]. For (**I**), HOMO and LUMO energies were -5.8001 eV and -2.0038 eV, respectively. This provides us an energy gap (ΔE) of ca. 3.7963 eV between the two orbitals. HOMO-LUMO energy gap is inversely related to the chemical stability of the molecule; therefore, the lower ΔE value indicates that the compound is more chemically reactive and electron transition sensitive [76]. This type of analysis plays a very important role in molecular electronics, photovoltaic materials, and prediction of biological activity. Particularly, the distribution of HOMO and LUMO in conjugated systems directly correlates with light absorption properties of the molecule [77]. Under this situation, localization of the HOMO solely on the phenolic ring suggests that it has the potential to be an electron donor, whereas localization of the LUMO around the imine group suggests that this region is prone to accepting an electron. These orbitals' transitions may influence the optoelectronic properties of the molecule and highlight its potential application in organic semiconductors or sensors [78]. Further, global reactivity descriptors derived using the HOMO-LUMO gap -electronegativity, chemical hardness, and softness - are available to predict the interaction of the molecule with other molecules.

3.3. Molecular Electrostatic Potential (MEP)

Information on the distribution of the charge density in a molecule and thus its chemical reactivity pattern is crucial for the prediction of how it will interact with other entities. Specifically, identification of potential electrophilic and nucleophilic attack sites enables the location of the molecule's reactive centers. One of the most commonly used methods for this is the MEP mapping, which is plotted on a constant electron density surface [79]. MEP maps allow for three-dimensional representation of a molecule's electrostatic pocket and depict probable distribution with different color codes. Blue regions are typically of maximum positive electrostatic potential (nucleophilic attack-susceptible regions), while red regions are of maximum negative potential (electrophilic attack-susceptible regions) [80]. In this study, the MEP map of (**I**) compound was plotted based on electrostatic potential values ranging from -6.280 a.u. to +6.280 a.u. (Fig. 2). Analysis of the map shows that the areas with the most negative potentials, red-coded, are localized over regions near the oxygen-containing hydroxyl group and imine group. This is an indication that these areas are susceptible to electrophilic attacks. Conversely, potential positives, which are colored in blue, represent the locations of possible positives and are mostly situated outside the thiophene ring. Visual and quantitative data from MEP analysis have proven to be valuable in predicting possible interaction mechanisms with biological targets, identification of ligand-receptor binding sites, and guiding drug design [81].

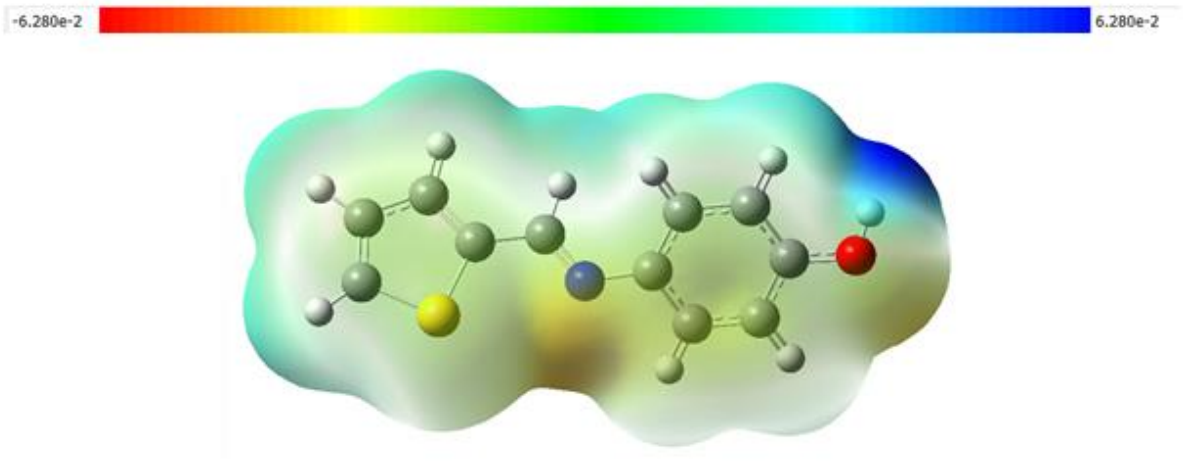

Fig. 2. MEP map of (I).

3.4. Non-Linear Optical (NLO) Properties

NLO properties, which impact the optical characteristics and stability of structures, are studied in fields such as physics, chemistry, biochemistry, and telecommunications [82]. Polarizability and hyperpolarizability values obtained from NLO calculations are necessary to measure the performance of the structure in these fields. NLO properties are important in the context that they not only determine the optical properties but also assist in confirming the presence of valence electrons within the material because valence electrons contribute with highest in polarizability and hyperpolarizability [83]. Urea is commonly employed as a reference compound in the literature when comparing dipole moment, polarizability, and hyperpolarizability values. Reported values for urea include a dipole moment of 1.3732 D, a polarizability of 3.8312 Å^3, and a hyperpolarizability of 3.7289 e.s.u. [84].

Table 2. Dipole moment, polarizability (a.u.), and hyperpolarizability (e.s.u.) of (I).

μ_x	**-0.3362**	**β_{xxx}**	**-2.2192×10^{-29}**
μ_y	1.1447	β_{xxy}	1.0709×10^{-30}
μ_z	0.0058	β_{xyy}	2.6966×10^{-31}
		β_{yyy}	4.6554×10^{-31}
α_{xx}	313.1891	β_{xxz}	-9.6091×10^{-31}
α_{xy}	-6.8212	β_{xyz}	1.4339×10^{-31}
α_{yy}	152.2924	β_{yyz}	-2.2556×10^{-31}
α_{xz}	1.8228	β_{xzz}	-5.8332×10^{-31}
α_{yz}	0.1161	β_{yzz}	6.6171×10^{-32}
α_{zz}	92.4615	β_{zzz}	13.7150×10^{-33}

When one examines Tables 2 and 3, one observes that the title compound exhibits greater polarizability and hyperpolarizability values than those of urea, in addition to its overall dipole moment.

Table 3. Average linear polarizability, polarizability anisotropy (Å^3), and hyperpolarizability (e.s.u.) values of (I).

Mean Linear Polarizability (α), (Å^3)	**27.57**
Polarizability Anisotropy (Δα), (Å^3)	85.80
Hyperpolarizability (β), (e.s.u.)	7.3×10^{-29}

3.5. Natural Bond Orbital (NBO) analysis

NBO analysis, based on the calculation of the shapes of orbitals in a molecular environment, was initially developed by Weinhold [85]. In order to define such orbital shapes, the single-electron density matrix is used, and bond formation is obtained through electron density shared between atoms [86]. Thus, NBO analysis takes a central position in computational chemistry as it provides information on bond formation nature and identifies donor and acceptor atoms based on electron density. The NBO analysis results are tabulated in Table 4. The values in Table 4 were obtained through second-order perturbation treatment of the Fock matrix [87]. E(2) values of 15 kcalmol^{-1} or greater are tabulated in Table 4.

Table 4. NBO analysis of the compound (I).

Donor (i)	Acceptor (j)	E(2) (kcalmol^{-1})	ε(j)- ε(i) (a.u.)	F(i,j) (a.u.)
BD(2) C4-C5	**BD*(2) C1-C6**	21.41	0.29	0.072
BD(2) C1-C6	**BD*(2) C4-C5**	19.09	0.27	0.065
BD(2) C1-C6	**BD*(2) C2-C3**	19.80	0.29	0.068
BD(2) C2-C3	**BD*(2) C14-C5**	22.22	0.27	0.071
BD(2) C2-C3	**BD*(2) C1-C6**	17.59	0.28	0.065
BD(2) C8-C9	**BD*(2) N1-C7**	19.50	0.30	0.069
BD(2) C8-C9	**BD*(2) C10-C11**	15.70	0.29	0.061
BD(2) C10-C11	**BD*(2) C8-C9**	**15.96**	**0.29**	**0.064**
LP(2) S1	**BD*(2) C8-C9**	22.25	0.26	0.068
LP(2) S1	**BD*(2) C10-C11**	**23.46**	0.25	0.071
LP(2) O1	**BD*(2) C4-C5**	**27.02**	0.35	0.093

In NBO analysis, high E(2) energy indicates good delocalization and stability. F(i,j) also rises linearly with E(2), a sign of a strong orbital interaction [88]. In the following, from Table 4, it is apparent that the largest intramolecular hyperconjugation occurs in n(O1)→π*(C4-C5) interaction. This interaction is revealed to enhance stability and possess good delocalization. A good interaction with excellent delocalization is also the n(S1)→π*(C10-C11) interaction.

3.6. Mulliken Charge Distribution

A common method for assessing the physical and chemical characteristics of a molecule is Mulliken charge analysis. By analyzing Mulliken charges, regions of positive and negative charge density within the structure are determined, which in turn determine electrophilic and nucleophilic regions [89]. Table 5 presents the Mulliken charge distribution for compound (**I**), which provides significant information regarding the electronic structure and potential reactive positions in the molecule. It is evident from the results that there are atoms with large negative charges, including the sulfur atom (S1) with a -0.324 charge and the oxygen atom (O1) with -0.244. These negative charge densities suggest that these atoms have the ability to act as nucleophilic sites and interactively as sites for electrophilic attack. Furthermore, they suggest that the carbon atom C7 bearing the imine linkage possesses a very high density of negative charge (-0.776) indicating a region of electron abundance with a possible effect on the reactivity of the molecule. Conversely, the carbon atom C9 carries the greatest positive charge (+1.002), which means it is electrophilic and most probably a target of nucleophilic attack. Other carbon atoms such as C4 (-0.513) and C10 (-1.060) also carry considerable negative charges and are yet more reflective of regions of electron density poised to add chemical activity to the molecule. The hydrogen atoms carry essentially minor positive charges, consistent with their role in bonding and relative electropositivity. Overall, the Mulliken charge distribution provides an accurate electron density map of the molecule, defining important nucleophilic and electrophilic positions. This is essential to the knowledge of chemical reactivity, interaction site for potential ligands, and overall stability of the compound. This information can be employed in guiding additional research in molecular interactions, catalysis, and biological function.

Table 5. Mulliken charges (a.u.) of the compound (I).

Atom	Charge	Atom	Charge
S1	-0.324265	C10	-1.059932
O1	-0.244303	C11	0.360001
N1	0.081367	H1	0.262708
C1	-0.047191	H2	0.166269
C2	-0.132624	H3	0.174105
C3	0.023799	H5	0.124312
C4	-0.512979	H6	0.131176
C5	0.105757	H7	0.039276
C6	-0.058659	H9	0.143941
C7	-0.775677	H10	0.124435
C8	0.167134	H11	0.249706
C9	1.001646		

3.7. Hirshfeld Surface Analysis

The Hirshfeld surface is used to determine the area occupied by a molecular structure within a crystal and divide the electron density in the crystal into different areas on the molecule [62]. The Hirshfeld surface analysis is a valuable resource for identifying intermolecular interactions within a molecule and understanding the modes of packing of crystals [90]. This analysis,

by means of several mapped surfaces, brings an improvement to understanding the molecule nature, the intermolecular contacts, and their effect on the overall structure. Fig. 3 presents the d_{norm} (a), shape index (b), and curvedness (c) maps for the title compound.

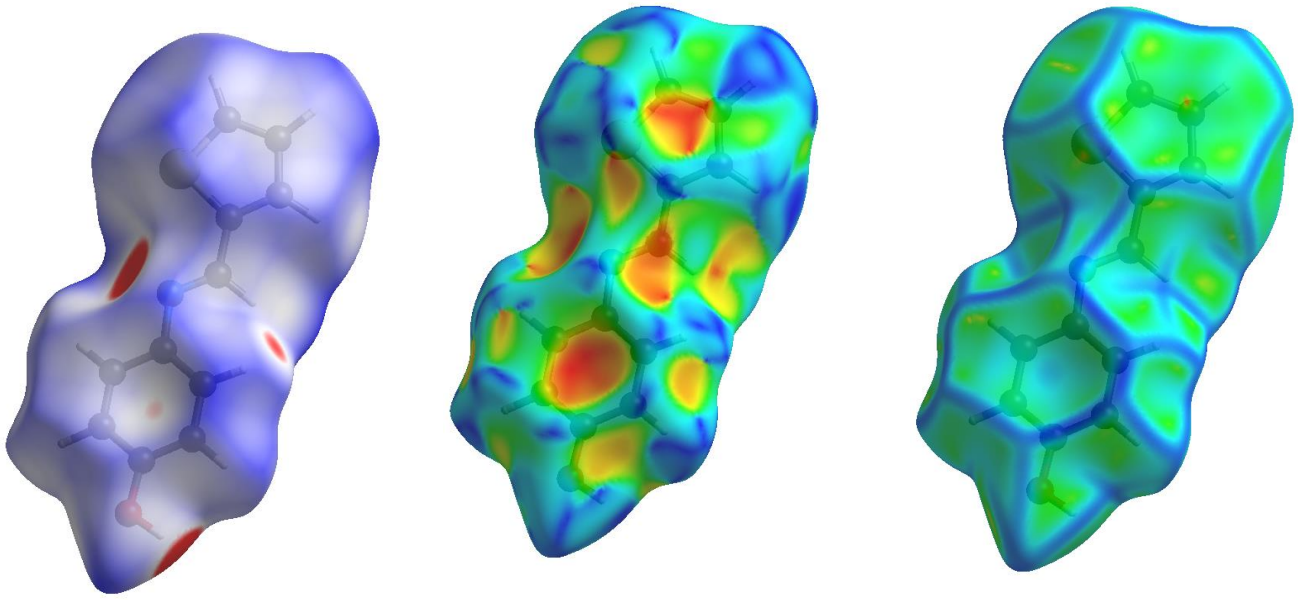

(a) **(b)** **(c)**

Fig. 3. d_{norm} (a), shape index (b) and curvature (c) maps of the title compound.

The d_{norm} map of a molecule is split into three different hues: red, blue, and white. Red represents negative d_{norm} values, which correspond to contacts below the sum of van der Waals radii. Blue regions represent positive d_{norm} values, *i.e.*, interactions greater than van der Waals radii, and white regions represent d_{norm} values near zero, *i.e.*, distances are approximately equal to the van der Waals radii. Fig. 3a presents the red spot map of the title compound in the range -0.2105-1.2515 a.u. On observation, there can be observed three large red spots. These regions correspond to the N1 atom involved in the imine bond, the hydrogen atom attached to the hydroxyl group of the benzene ring, and the hydrogen atom attached to C7 involved in the imine bond. The shape index map of the title compound plotted between -0.9970 and 0.9982 a.u. is illustrated in Fig. 3b. The shape index map includes red and blue triangles in which ring atoms on the molecular surface are marked and reveal π-π stacking interactions within the molecule [91]. Notably, the distinct red triangles are observed over the C11 atom of the thiophene ring and the C7 atom belonging to the imine bond. The curvedness map depicted in Fig. 3c is plotted between -4.0298 and 0.3226 a.u. In curvedness maps, broad and flat regions enclosed by blue lines can be easily identified as π-π interaction regions [92]. The curvedness map of the title compound recognizes these large, flat blue regions limited mostly on the N1 atom within the imine ring, as well as regions corresponding to hydrogen atoms attached to C-H bonds.

A second map that is obtained from the Hirshfeld surface analysis and displays the contacts within the molecule is the 2D fingerprint plot. Fig. 4 illustrates these plots.

The normal right and left wing look of the Hirshfeld surface is a sign of the presence of C–H…π interactions within the structure. This is also validated by the shape index map. The interactions also show up in the fingerprint plots of all intermolecular contacts and the C…H/H…C interactions specifically. This discovery also indicates the presence of free π electrons within the structure. Furthermore, the two large spikes of the 2D fingerprint plots are actually referring to N–H interactions [90]. This can be observed both in the fingerprint plot of all the intermolecular contacts and in the fingerprint plot for N…H/H…N contacts. The contributions of the various intermolecular interactions in the molecule are the following: H…H/H…H with 32.6%, C…H/H…C with 27.3%, S…H/H…S with 15.4%, N…H/H…N with 9.3%, O…H/H…O with 9.1%, C…C with 6.0%, S…O with 0.2%, and S…C with 0.1%. A pie chart that represents these percentages is also shown in Fig. 4.

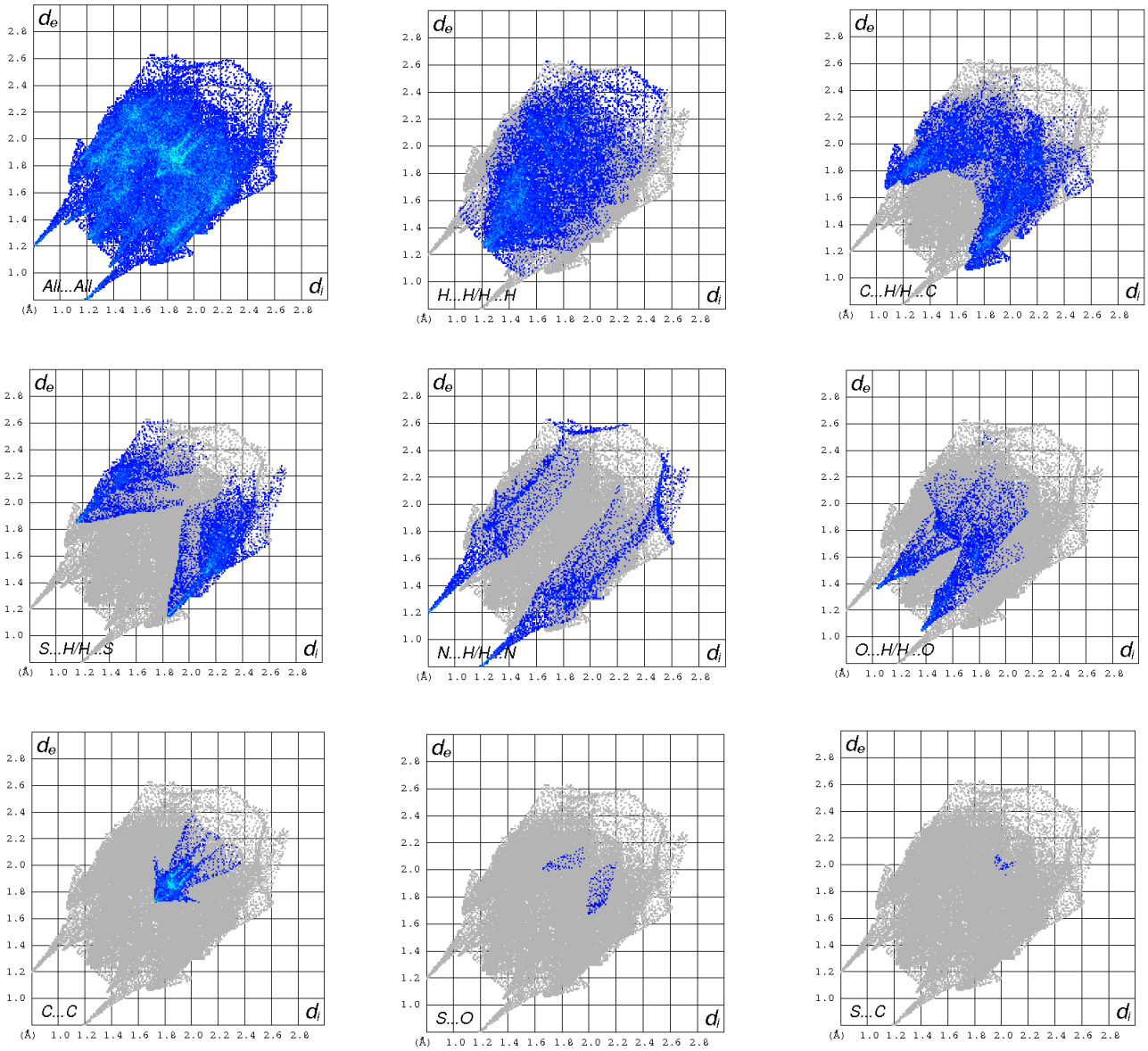

Fig. 4. 2D fingerprint maps of (I).

3.8. Molecular Docking Simulation

Molecular docking is a computational method employed to model the interaction between a small-molecule ligand and a macromolecular target [92]. Especially in drug development, simulating the binding of candidate molecules to target locations is cost-effective and to reduce the number of candidates to experimental evaluation. During docking, some scoring functions are utilized to estimate the binding affinity between the target and the ligand [93]. Low binding affinity is indicative of strong protein-ligand interactions, and high binding affinity is an indicator of weak binding. The binding affinity is enhanced through interactions such as hydrogen bonds, hydrophobic contacts, and so on between the ligand and protein [93]. Molecular docking is similar to experimental high-throughput screening (HTS) methods in being faster and cheaper in screening [94]. This strategy is applied widely not only for the discovery of new leads of drugs but also for drug repurposing, multi-target directed drug design, and the prediction of potential side effects [95]. In this paper, the title compound was prepared as a ligand and its antiviral, anticancer, and anti-Alzheimer activity was determined against Ebola virus, c-KIT protein, and acetylcholinesterase enzyme, respectively. Table 6 illustrates the ligand-protein interaction, whereas Fig.s 5.a, 5.b, and 5.c illustrate the 3D and 2D view of Ebola virus-ligand, c-KIT-ligand, and acetylcholinesterase-ligand interaction, respectively.

It is observed from Table 6 and Fig. 5 that the interaction and binding affinities are consistent in each system. For the Ebola virus protein-ligand interaction, amino acid residues Ile-295, Pro-293, and Lys-248 participate. For c-KIT-ligand interaction, protein residues Val-654, Cys-809, and Lys-623 participate, while for the acetylcholinesterase enzyme-ligand interaction, enzyme residues Phe-330 and Trp-84 participate in hydrophobic interaction. These hydrophobic interactions are due to exclusion of water in the apolar areas between protein and ligand, which makes binding stable by stabilizing the ligand in its binding pocket [96].

Table 6. Protein-ligand interaction data for the title compound.

Protein	Bonding Affinity (kcal mol^{-1})	Hydrophobic Interaction	Hydrogen Bond Interaction
Ebola virus (4ibb)	-5.3	Ile-295 Pro-293 Lys-248	His-296
c-KIT (4u0i)	-7.3	Cys-809 Lys-623 Val-654	Glu-640 Asp-810
Acetylcholinesterase (1qti)	-7.0	Phe-330 Trp-84	Gly-441 His-440 Glu-199

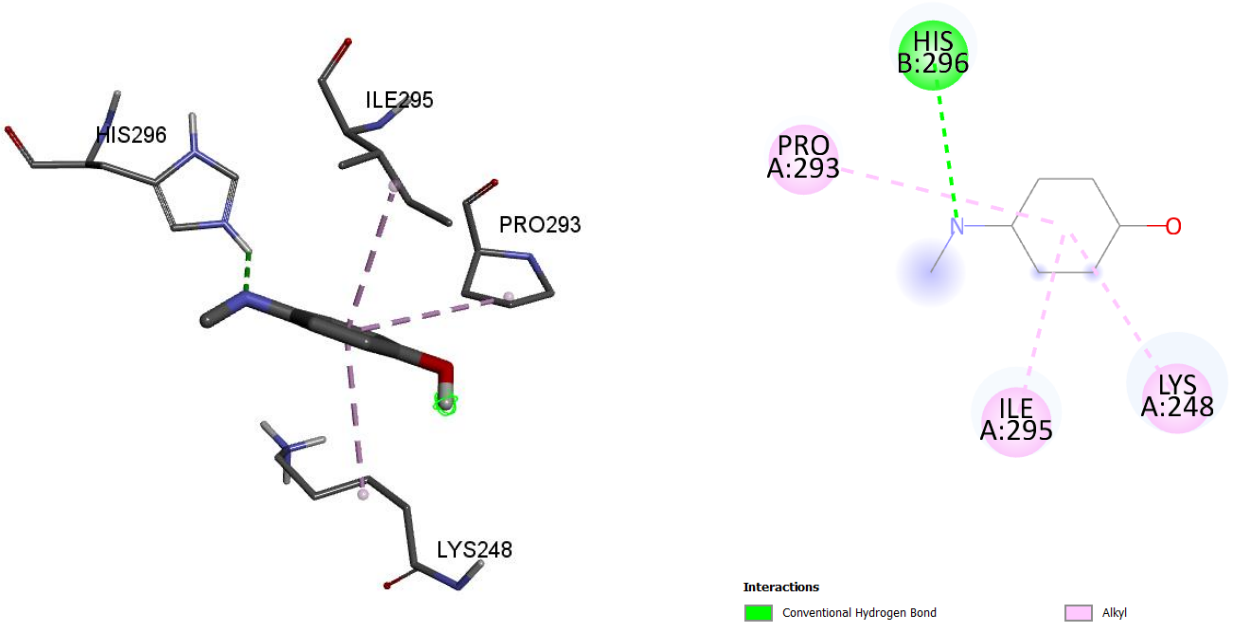

(a)

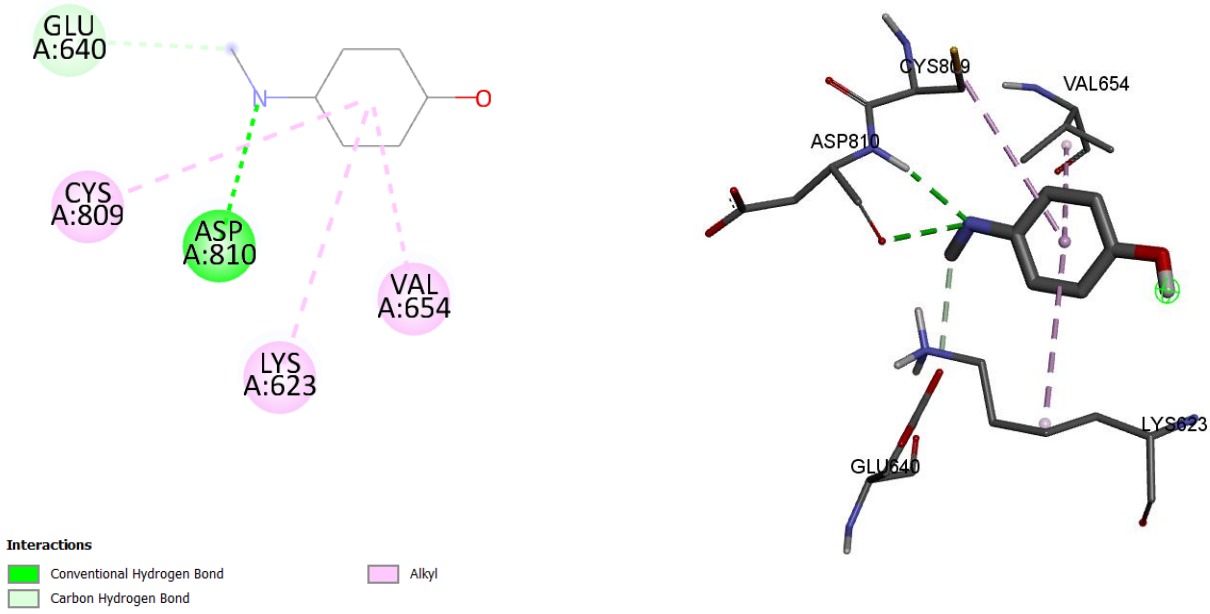

(b)

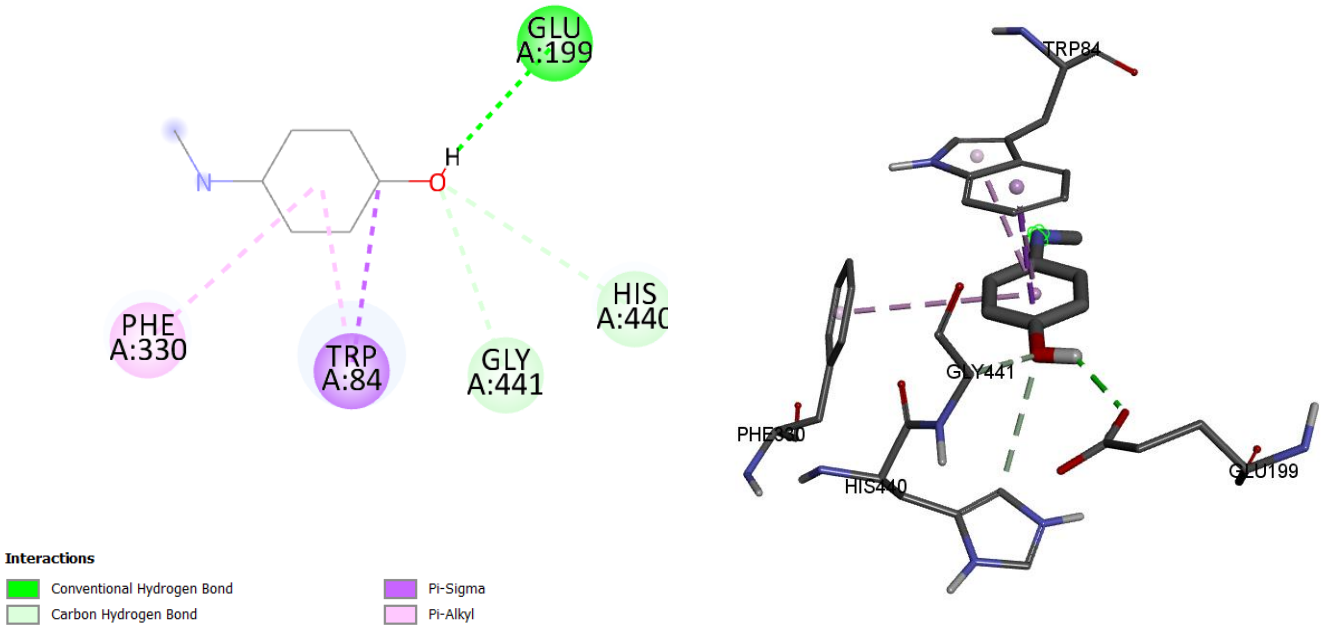

(c)

Fig. 5. (a) Ebola virüs protein-ligand (b) c-KIT-ligand (c) acetylcholinesterase enzyme-ligand interactions of (I).

Hydrogen bonding is a key type of interaction in protein-ligand complexes that plays a central role in binding site region identification and binding energy optimization [97]. In the Ebola virus protein-ligand complex, the hydrogen atom from the imidazole ring of the His-296 amino acid residue participates in an N-H···N hydrogen bond with the N1 atom from the ligand's imine group. In this interaction, hydrogen in the imidazole is the donor, and the N1 atom in the imine group is the acceptor. The bond distance of this hydrogen interaction was found to be 2.79 Å. In the ligand–c-KIT protein interaction, the C7 atom of the ligand belonging to the imine bond engages in the C–H···O hydrogen bond with the oxygen atom of the Glu-640 amino acid residue's carboxyl group. The calculated bond length was 3.51 Å. During this interaction, the C7 atom in the imine ring was the donor of the hydrogen bond, and the Glu-640 acted as the acceptor. Also, an N–H···O interaction was observed between the N1 atom of the imine ring of the ligand and the oxygen atom in residue Asp-810 with a bond distance of 3.31 Å. The N1 atom is the donor and the oxygen atom in Asp-810 is the acceptor. Finally, in the same protein-ligand complex, an N–H···N hydrogen bond was discovered between the N1 atom of the imine ring of the ligand and the amide hydrogen of Asp-810. This is a 2.40 Å hydrogen bond, wherein the amide hydrogen of Asp-810 is the donor and the N1 atom is the acceptor. In the interaction of the ligand with acetylcholinesterase enzyme, H1 atom of the ligand responsible for –OH (hydroxyl) group forms C–H···O interaction with oxygen atom of Glu-199 amino acid residue. Bond distance was determined to be 2.20 Å. The H1 atom acts as the donor and oxygen atom of Glu-199 as the acceptor in the interaction. In addition, a C–H···O interaction was observed between the carbon atom of the His-440 residue and the O1 atom of the ligand. This bond distance was calculated to be 3.78 Å, where the O1 atom was the donor and the carbon atom of the His-440 residue was the acceptor. Besides, another C–H···O interaction was discovered between the Gly-441 residue carbon atom and the O1 atom of the ligand with a distance of 3.18 Å. The donor is the Gly-441 carbon atom, and the acceptor is the O1 atom. All information for these interactions is presented in Table 7.

Table 7. Molecular docking-based hydrogen bonding interaction data.

Hydrogen Bond	Donor	Acceptor	Bond Length (Å)	Interaction Type
His-296-N1	His-296	N1	2.79	N-H…N
Glu-640-C7	C7	Glu-640	3.51	C-H…O
Asp-810-N1	N1	Asp-810	3.39	N-H…O
Asp810-N1	Asp-810	N1	2.40	N-H…N
Glu-199-H1	H1	Glu-199	2.20	C-H…O
His-440-O1	O1	His-440	3.78	C-H…O
Gly-441-O1	Gly-441	O1	3.18	C-H…O

3.9. ADME-Tox Study

Absorption, Distribution, Metabolism, Excretion, and Toxicity (ADME-Tox) parameters play a crucial role in drug development, as they inform the design of new drug candidates and assist in establishing appropriate dosage, dosing intervals,

and safety criteria throughout the treatment period [98]. The minimum effective dose depends on the drug's receptor affinity and its activity at the binding site. Thus, identifying the minimum dose and pharmacokinetic characteristics of candidate molecules is crucial to assess their efficacy [99]. The patient's optimal response from the daily dose given and sustaining this dose all day long correlate with the distribution characteristics of the drug [100]. Further, metabolism and excretion factors are significant in assessing toxicity, as accumulation of the drug molecule within the liver can interfere with metabolic elimination patterns [101]. Absorption can be defined as the process of a drug being conveyed to systemic circulation [99]. The drug's absorption in the body is equally important as binding to the active receptor site because poor absorption reduces the potential of the drug to yield the desired molecular effect [102]. Several key factors regulate the ADME-Tox characteristics of a drug candidate, including lipophilicity, aqueous solubility, pharmacokinetic properties, and drug-likeness. Lipophilicity is an important parameter in lead discovery and lead optimization of drug candidates as it is one of the most informative physicochemical properties regarding structure and activity of therapeutic chemicals [103]. Lipophilicity also affects pharmacodynamic and toxicologic activity [104]. Solubility is a function of lipophilicity and can be described by function of log P and melting point [105]. Based on currently used drugs and candidate molecules, it is widely accepted that molecules with lipophilicity values (log P) greater than 5 tend to undergo rapid metabolic degradation, have low solubility, and exhibit poor absorption [106,107]. Lipinski suggests that molecules with lipophilicity values below 5 should proceed to phase II trials. This concept is known as Lipinski's Rule of Five [107]. Lipinski identified four critical parameters affecting absorption and solubility: molecular weight, log P, hydrogen bond donors, and hydrogen bond acceptors. Cut-off values for these parameters are at 5 or their multiples. Based on this, Lipinski has explained that a drug candidate molecule with more than 5 hydrogen bond donors, more than 10 hydrogen bond acceptors, molecular weight more than 500, and log P more than 5 is going to have poor absorption [107]. Physicochemical and pharmacokinetic features of the title compound are summarized in Table 8, while drug-likeness features of the title compound are presented in Table 9.

Table 8. Physicochemical and pharmacokinetic properties of the title compound.

Property	Value
Number of Hydrogen Bond Acceptors	2
Number of Hydrogen Bond Donors	1
Total Polar Surface Area (TPSA)	60.83 Å
Lipophilicity (log P)	2.15
Water Solubility (log S)	-3.36
GI Absorption	High
KBB Transition	Yes
CYP1A2 Inhibitor	Yes
CYP2C19 Inhibitor	Yes
CYP2C9 Inhibitor	No
CYP2D6 Inhibitor	No
CYP3A4 Inhibitor	No
Log Kp (skin permeability)	-5.50 $cm.s^{-1}$

When Table 8 is examined, the log P value, the number of hydrogen bond acceptors, and the number of hydrogen bond donors comply with Lipinski's Rule of Five [107]. The log S value is -3.36, indicating a moderate level of water solubility. Solubility is an important parameter for a drug candidate, and log S values below -4 are generally considered acceptable thresholds [108]. The GI absorption is satisfactory and as per both TPSA and log P values. The molecule satisfies all Lipinski, Veber, Ghose, Egan, and Muegge rules. The title compound permeates through the blood-brain barrier and also inhibits CYP1A2 and CYP2C19 enzymes. The log Kp value is low in relation to other values, indicating that the compound is less permeable via the skin.

Table 9. Drug similarity data for the title compound.

Property	Value
Lipinski	Yes
Ghose	Yes
Veber	Yes
Egan	Yes
Muegge	Yes
Bioavailability	0.55

4. Conclusions

In this study, the structural, electronic, and biological properties of the Schiff base compound 2-[(4-hydroxyphenyl)iminomethyl]thiophene were comprehensively investigated using quantum chemical calculations and molecular docking simulations. The results provided significant insights into the compound's potential as a drug-like molecule. Geometry optimization, performed using DFT calculations, revealed a stable molecular structure characterized by planarity in the aromatic systems and effective conjugation between the thiophene and imine groups. The optimized geometry also supported the presence of intramolecular hydrogen bonding, contributing to the overall stability of the molecule. FMO analysis indicated a moderate HOMO–LUMO energy gap, suggesting good chemical reactivity and kinetic stability. The mapped MEP highlighted the imine nitrogen (N1) and hydroxyl oxygen (O1) as key reactive centers, with NBO analysis confirming the presence of strong donor–acceptor interactions and hyperconjugation effects that enhance the molecule's stability and reactivity. NLO analysis revealed that the compound exhibits significantly higher polarizability and hyperpolarizability compared to the urea standard, indicating its suitability for optoelectronic applications. Hirshfeld surface analysis provided further confirmation of the molecule's stable packing and significant intermolecular interactions, particularly hydrogen bonding and π–π stacking, which influence its crystal behavior and solid-state stability. Molecular docking studies were conducted to evaluate the biological potential of the compound against three targets: the tyrosine kinase receptor c-KIT (associated with cancer), the Ebola virus glycoprotein, and human acetylcholinesterase (AChE, associated with Alzheimer's disease). The docking results demonstrated favorable binding affinities and key interactions with active site residues, such as hydrogen bonding with Glu640 in c-KIT, hydrophobic interactions with GP1 subunits in EBOV, and π–π stacking with Trp86 and Tyr337 in AChE. These interactions suggest that the compound could inhibit target proteins effectively. ADME-Tox analysis revealed that the compound possesses favorable pharmacokinetic properties, including high predicted oral bioavailability, good gastrointestinal absorption, and no violation of Lipinski's rule of five. Additionally, the compound was predicted to be non-mutagenic, non-carcinogenic, and have low predicted toxicity risks, supporting its potential as a safe therapeutic agent.

In summary, the study demonstrates that 2-[(4-hydroxyphenyl)iminomethyl]thiophene is a chemically stable and biologically active compound with promising drug-like properties. Its anticancer, antiviral, and anti-Alzheimer activities, supported by docking and ADME-Tox data, indicate its potential as a candidate for future drug development efforts and preclinical evaluation.

References

[1] H. Schiff, "Investigations on salicyl derivatives," *Justus Liebigs Annalen der Chemie*, vol. 150, no. 2, pp. 193-200, 1869.

[2] R. Meena, P. Meena, A. Kumari, N. Sharma, and N. Fahmi, "Schiff Base in Organic, Inorganic and Physical Chemistry," in *Schiff Bases and Their Metal Complexes: Synthesis, Structural Characteristics and Applications*, T. Akitsu, Ed. IntechOpen, 2023. doi: 10.5772/intechopen.108396.

[3] Z. Hussain, E. Yousif, A. Ahmed, and A. Altaie, "Synthesis and characterization of Schiff's bases of sulfamethoxazole," *Organic and Medicinal Chemistry Letters*, vol. 4, no. 1, pp. 1-4, 2014. doi: 10.1186/2191-2858-4-1.

[4] S. L. Sangle, "Introduction to Schiff base," in *Schiff Base in Organic, Inorganic and Physical Chemistry*, T. Akitsu, Ed. IntechOpen, 2022. doi: 10.5772/intechopen.104134.

[5] S. K. Raju, A. Settu, A. Thiyagarajan, D. Rama, P. Sekar, and S. Kumar, "Biological applications of Schiff bases: An overview," *GSC Biological and Pharmaceutical Sciences*, vol. 21, no. 3, pp. 203-215, 2022. doi: 10.30574/gscbps.2022.21.3.0484.

[6] A. M. Abu-Dief, M. Ibrahim, and A. Mohamed, "A review on versatile applications of transition metal complexes incorporating Schiff bases," *Beni-Suef University Journal of Basic and Applied Sciences*, vol. 4, no. 2, pp. 119-133, 2015. doi: 10.1016/j.bjbas.2015.05.004

[7] F. Tisato, F. Refosco, and G. Bandoli, "Structural survey of technetium complexes," *Coordination Chemistry Reviews*, vol. 135–136, pp. 325-397, 1994. doi: 10.1016/0010-8545(94)80072-3

[8] A. L. Berhanu, M. Gaurav, I. Mohiuddin, A. K. Malik, J. S. Aulakh, V. Kumar, and K. H. Kim, "A review of the applications of Schiff bases as optical chemical sensors," *Trends in Analytical Chemistry*, vol. 116, pp. 74-91, 2019. doi: 10.1016/j.trac.2019.04.025

[9] S. A. Dalia, F. Afsan, M. S. Hossain, M. N. Khan, C. Zakaria, M. E. Zahan, and M. Ali, "A short review on chemistry of Schiff base metal complexes and their catalytic application," *International Journal of Chemical Studies*, vol. 6, no. 3, pp. 2859-2866, 2018.

[10] C. C. Ersanlı and S. Başak, "Quantum Mechanical Calculations and Molecular Docking Simulation Studies of N-(5-chloro-2-oxobenzyl)-2-hydroxy-5-methylanilinium Compound," *International Scientific and Vocational Studies Journal*, vol. 8, no. 2, pp. 162-177, 2024. doi: 10.47897/bilmes.1573560

[11] H. M. Alkahtani, A. A. Almehizia, M. A. Al-Omar, A. J. Obaidullah, A. A. Zen, A. S. Hassan, and W. M. Aboulthana, "In vitro evaluation and bioinformatics analysis of Schiff bases bearing pyrazole scaffold as bioactive agents: Antioxidant, anti-diabetic, anti-Alzheimer, and anti-arthritic activities," *Molecules*, vol. 28, no. 20, p. 7125, 2023. doi: 10.3390/molecules28207125

[12] T. Alorini, I. Daoud, A. N. Al-Hakimi, F. Alminderej, and A. E. Albadri, "An experimental and theoretical investigation of antimicrobial and anticancer properties of some new Schiff base complexes," *Research on Chemical Intermediates*, vol. 49, no. 4, pp. 1701-1730, 2023. doi: 10.1007/s11164-022-04946-1

[13] Y. Gou, J. Li, B. Fan, B. Xu, M. Zhou, and F. Yang, "Structure and biological properties of mixed-ligand Cu(II) Schiff base complexes as potential anticancer agents," *European Journal of Medicinal Chemistry*, vol. 134, pp. 207-217, 2017. doi: 10.1016/j.ejmech.2017.03.022

[14] M. Köse, G. Ceyhan, M. Tümer, İ. Demirtaş, İ. Gönül, and V. McKee, "Monodentate Schiff base ligands: Structural characterization, photoluminescence, anticancer, electrochemical, and sensor properties," *Spectrochimica Acta Part A: Molecular and Biomolecular Spectroscopy*, vol. 137, pp. 477-485, 2015. doi: 10.1016/j.saa.2014.08.124

[15] A. Garg, D. Dureja, A. Vijeata, G. R. Chaudhary, S. Berry, S. Chaudhary, and A. Bhalla, "Synthesis of novel α-carboxylate-β-bismethylsulfanyl pyrazolyl Schiff base derivatives: Targeting DNA gyrase for antibacterial activity," *Journal of Molecular Structure*, vol. 1337, p. 141954, 2025. doi: 10.1016/j.molstruc.2025.141954

[16] N. Isalm *et al*., "Exploration of the synthesis, crystal structure, Hirshfeld surface analysis, binding properties, antibacterial activities, and molecular docking of a Schiff base nickel(II) complex," *Journal of Molecular Structure*, vol. 140294, 2024. doi: 10.1016/j.molstruc.2024.140294

[17] H. A. Hasan, S. M. Mahdi, and H. A. Ali, "Tetradentate azo Schiff base Ni(II), Pd(II), and Pt(II) complexes: Synthesis, spectral properties, antibacterial activity, cytotoxicity, and docking studies," *Bulletin of the Chemical Society of Ethiopia*, vol. 38, no. 1, pp. 99-111, 2024. doi: 10.4314/bcse.v38i1.7

[18] D. Pardaeva *et al*., "Spectral characterization and antibacterial, antifungal, antiviral activities of salicyl-based new Schiff bases and their Co(II), Ni(II), Cu(II), Zn(II), and Pd(II) complexes," *Revue Roumaine de Chimie*, vol. 69, no. 1-2, pp. 83-96, 2024. doi: 10.33224/rrch.2024.69.1-2.10

[19] M. Azzouzi *et al*., "Synthesis, crystal structure, and antiviral evaluation of new imidazopyridine-Schiff base derivatives: In vitro and in silico anti-HIV studies," *RSC Advances*, vol. 14, no. 50, pp. 36902–36918, 2024. doi: 10.1039/d4ra07561g

[20] R. H. Taha *et al*., "Impact of Fe(III) and Ce(III) ions on pharmacological properties of novel Schiff base ligand: Anticancer, antiviral, antioxidant, antifungal investigations and computational insights," *Journal of Molecular Liquids*, vol. 427, p. 127382, 2025. doi: 10.1016/j.molliq.2024.127382

[21] M. Sarfraz *et al*., "New pyrimidinone-bearing aminomethylenes and Schiff bases as potent antioxidant, antibacterial, SARS-CoV-2, and COVID-19 main protease (MPro) inhibitors: Design, synthesis, bioactivities, and computational studies," *ACS Omega*, vol. 9, no. 24, pp. 25730-25747, 2024. doi: 10.1021/acsomega.3c09393

[22] M. Yılmaz, "Cancer epidemiology," in *Cancer Genetics and Molecular Biology*, İ. Değirmenci, Ed. Istanbul: Nobel, 2022, pp. 3-25.

[23] Özbayer, "Carcinogenesis," in *Cancer Genetics and Molecular Biology*, İ. Değirmenci, Ed. Istanbul: Nobel, 2022, pp. 29-47.

[24] R. Robinson, Y. M. Wu, and S. F. Lin, "The protein tyrosine kinase family of the human genome," *Oncogene*, vol. 19, no. 49, pp. 5548-5557, 2000. doi: 10.1038/sj.onc.1204082

[25] F. Inizan, M. Hanna, M. Stolyarchuk, I. Chauvot de Beauchêne, and L. Tchertanov, "The first 3D model of the full-length KIT cytoplasmic domain reveals a new look for an old receptor," *Scientific Reports*, vol. 10, no. 1, p. 5401, 2020. doi: 10.1038/s41598-020-62352-2

[26] P. Besmer, J. Murphy, P. George, *et al*., "A new acute transforming feline retrovirus and relationship of its oncogene v-kit with the protein kinase gene family," *Nature*, vol. 320, pp. 415-421, 1986. doi: 10.1038/320415a0

[27] D. Mol, D. R. Dougan, T. R. Schneider, R. J. Skene, M. L. Kraus, D. N. Scheibe, *et al*., "Structural basis for the autoinhibition and STI-571 inhibition of c-Kit tyrosine kinase," *J. Biol. Chem.*, vol. 279, no. 30, pp. 31655-31663, 2004. doi: 10.2210/pdb1t46/pdb

[28] Sheikh, T. Tran, S. Vranic, A. Levy, and R. D. Bonfil, "Role and significance of c-KIT receptor tyrosine kinase in cancer: A review," *Bosn. J. Basic Med. Sci.*, vol. 22, no. 5, p. 683, 2022. doi: 10.17305/bjbms.2022.7185

[29] J. Lennartsson and L. Rönnstrand, "Stem cell factor receptor/c-Kit: From basic science to clinical implications," *Physiol. Rev.*, vol. 92, no. 4, pp. 1619-1649, 2012. doi: 10.1152/physrev.00046.2011

[30] M. Abbaspour Babaei, B. Kamalidehghan, M. Saleem, H. Z. Huri, and F. Ahmadipour, "Receptor tyrosine kinase (c-Kit) inhibitors: A potential therapeutic target in cancer cells," *Drug Des. Devel. Ther.*, vol. 10, pp. 2443-2459, 2016. doi: 10.2147/DDDT.S106527

[31] J. A. Curtin, K. Busam, D. Pinkel, and B. C. Bastian, "Somatic activation of KIT in distinct subtypes of melanoma," *J. Clin. Oncol.*, vol. 24, no. 26, pp. 4340-4346, 2006. doi: 10.1200/JCO.2005.03.9199

[32] A. Beghini, C. B. Ripamonti, R. Cairoli, G. Cazzaniga, P. Colapietro, F. Elice, *et al*., "KIT activating mutations: Incidence in adult and pediatric acute myeloid leukemia, and identification of an internal tandem duplication," *Haematologica*, vol. 89, no. 8, pp. 920-925, 2004. [Online]. Available: https://pubmed.ncbi.nlm.nih.gov/15339674

[33] D. Malvy, A. K. McElroy, H. de Clerck, S. Günther, and J. van Griensven, "Ebola virus disease," *Lancet*, vol. 393, no. 10174, pp. 936-948, 2019. doi: 10.1016/S0140-6736(18)33132-5

[34] T. Q. Lo, B. J. Marston, B. A. Dahl, and K. M. De Cock, "Ebola: Anatomy of an epidemic," *Annu. Rev. Med.*, vol. 68, no. 1, pp. 359-370, 2017. doi: 10.1146/annurev-med-050715-105505

[35] T. Garske, A. Cori, A. Ariyarajah, I. M. Blake, I. Dorigatti, T. Eckmanns, *et al*., "Heterogeneities in the case fatality ratio in the West African Ebola outbreak 2013–2016," *Philos. Trans. R. Soc. Lond. B Biol. Sci.*, vol. 372, no. 1721, p. 20160308, 2017. doi: 10.1098/rstb.2016.0308

[36] S. Baize, D. Pannetier, L. Oestereich, T. Rieger, L. Koivogui, N. Magassouba, *et al*., "Emergence of Zaire Ebola virus disease in Guinea," *N. Engl. J. Med.*, vol. 371, no. 15, pp. 1418-1425, 2014. doi: 10.1056/NEJMoa1404505

[37] H. Feldmann and T. W. Geisbert, "Ebola hemorrhagic fever," *Lancet*, vol. 377, no. 9768, pp. 849-862, 2011. doi: 10.1016/S0140-6736(10)60667-8

[38] Almeida-Pinto, R. Pinto, and J. Rocha, "Navigating the complex landscape of Ebola infection treatment: A review of emerging pharmacological approaches," *Infect. Dis. Ther.*, vol. 13, pp. 21-55, 2024. doi: 10.1007/s40121-023-00913-y

[39] M. U. Mirza, M. Vanmeert, A. Ali, K. Iman, M. Froeyen, and M. Idrees, "Perspectives towards antiviral drug discovery against Ebola virus," *J. Med. Virol.*, vol. 91, no. 12, pp. 2029-2048, 2019. doi: 10.1002/jmv.25357

[40] U. Saray and U. Çavdar, "Investigating the role of artificial intelligence in the diagnosis and treatment of Alzheimer's disease," in *VIII International Scientific and Vocational Studies Congress (BILMES 2023), Turkey*, Dec. 2023, pp. 132-137.

[41] Vecchio, L. Sorrentino, A. Paoletti, R. Marra, and M. Arbitrio, "The state of the art on acetylcholinesterase inhibitors in the treatment of Alzheimer's disease," *J. Cent. Nerv. Syst. Dis.*, vol. 13, 11795735211029113, 2021. doi: 10.1177/11795735211029113

[42] C. P. Ferri, M. Prince, C. Brayne, H. Brodaty, L. Fratiglioni, M. Ganguli, *et al*., "Global prevalence of dementia: a Delphi consensus study," *Lancet*, vol. 366, no. 9503, pp. 2112-2117, 2005. doi: 10.1016/S0140-6736(05)67889-0

[43] E. Bomasang-Layno and R. Bronsther, "Diagnosis and treatment of Alzheimer's disease: An update," *Delaware J. Public Health*, vol. 7, no. 4, pp. 74-85, 2021. doi: 10.32481/djph.2021.09.009

[44] Hampel, M. M. Mesulam, A. C. Cuello, A. S. Khachaturian, A. Vergallo, M. R. Farlow, *et al*., "Revisiting the Cholinergic Hypothesis in Alzheimer's Disease: Emerging Evidence from Translational and Clinical Research," *J. Prev. Alzheimers Dis.*, vol. 6, no. 1, pp. 2-15, 2019. doi: 10.14283/jpad.2018.43

[45] B. Ul Islam and S. Tabrez, "Management of Alzheimer's disease-An insight into enzymatic and other novel potential targets," *Int. J. Biol. Macromol.*, vol. 97, pp. 700-709, 2017. doi: 10.1016/j.ijbiomac.2016.12.074

[46] S. López, J. Bastida, F. Viladomat, and C. Codina, "Acetylcholinesterase inhibitory activity of some Amaryllidaceae alkaloids and Narcissus extracts," *Life Sci.*, vol. 71, no. 21, pp. 2521-2529, 2002. doi: 10.1016/S0024-3205(02)02034-9

[47] V. F. Echenique, G. Alvarez-Rivera, V. M. A. Luna, A. F. V. da Cruz Antonio, M. R. Mazalli, E. Ibañez, *et al*., "Pressurized liquid extraction with ethanol in an intermittent process for rice bran oil: Evaluation of process variables on the content of β-sitosterol and phenolic compounds, antioxidant capacity, acetylcholinesterase inhibitory activity, and oil quality," *LWT – Food Sci. Technol.*, vol. 207, p. 116650, 2024. doi: 10.1016/j.lwt.2023.116650

[48] C. Kazak, M. Aygün, G. Turgut Cin, M. Odabaşoğlu, S. Özbey, and O. Büyükgüngör, "2-[(4-Hydroxyphenyl)iminomethyl]thiophene," *Acta Crystallogr. Sect. C Struct. Chem.*, vol. 56, pt. 8, pp. 1044-1045, 2000. doi: 10.1107/S0108270100007770

[49] C. A. Lane, J. Hardy, and J. M. Schott, "Alzheimer's disease," *Eur. J. Neurol.*, vol. 25, no. 1, pp. 59-70, 2018. doi: 10.1111/ene.13439

[50] Ali, A. Haque, K. Saleem, and M.-F. Hsieh, "Schiff bases: An emerging class of therapeutic agents," *Curr. Org. Chem.*, vol. 20, no. 8, pp. 1-13, 2016. doi: 10.2174/1385272820666151123150433

[51] A. Tiwari, V. Gupta, and A. Kushwah, "In silico and in vitro anti-Alzheimer potential of Schiff base derivatives," *Med. Chem. Res.*, vol. 29, no. 5, pp. 813-822, 2020. doi: 10.1007/s00044-020-02551-y

[52] Matsuno, A. Marzi, and H. Feldmann, "Ebola virus entry: From molecular characterization to drug discovery," *Trends Microbiol.*, vol. 27, no. 7, pp. 593-604, 2019. doi: 10.1016/j.tim.2019.02.005

[53] S. M. Gomha, S. M. Riyadh, S. A. Alharbi, and M. M. Elaasser, "Synthesis and antiviral evaluation of new Schiff base derivatives against hepatitis A and Ebola viruses," *Arch. Pharm.*, vol. 355, no. 8, p. e2100509, 2022. doi: 10.1002/ardp.202100509

[54] Gaussian 03, Gaussian, Inc., Wallingford, CT, 2004. [Online]. Available: https://gaussian.com/

[55] P. J. Stephens, F. J. Devlin, C. F. Chabalowski, and M. J. Frisch, "Ab initio calculation of vibrational absorption and circular dichroism spectra using density functional force fields," *J. Phys. Chem.*, vol. 98, no. 45, pp. 11623-11627, 1994. doi: 10.1021/j100096a001

[56] A. D. Becke, "Density-functional thermochemistry. III. The role of exact exchange," *J. Chem. Phys.*, vol. 98, no. 7, pp. 5648-5652, 1993. doi: 10.1063/1.464913

[57] C. Lee, W. Yang, and R. G. Parr, "Development of the Colle-Salvetti correlation-energy formula into a functional of the electron density," *Phys. Rev. B*, vol. 37, no. 2, pp. 785-789, 1988. doi: 10.1103/PhysRevB.37.785

[58] G. A. Petersson and M. A. Al-Laham, "A complete basis set model chemistry. II. Open-shell systems and the total energies of the first-row atoms," *J. Chem. Phys.*, vol. 94, no. 9, pp. 6081-6090, 1991. doi: 10.1063/1.460447

[59] J. Frisch, A. B. Nielsen, and A. J. Holder, *GaussView user manual*. Gaussian Inc., 2001.

[60] J. Turner, J. J. McKinnon, S. K. Wolff, D. J. Grimwood, P. R. Spackman, D. Jayatilaka, and M. A. Spackman, "CrystalExplorer17 [Computer software]," Univ. Western Australia, 2017.

[61] F. L. Hirshfeld, "Bonded-atom fragments for describing molecular charge densities," *Theor. Chim. Acta*, vol. 44, no. 2, pp. 129-138, 1977. doi: 10.1007/BF00549096

[62] A. Spackman and D. Jayatilaka, "Hirshfeld surface analysis," *CrystEngComm*, vol. 11, no. 1, pp. 19-32, 2009. doi: 10.1039/B818330A

[63] J. McKinnon, D. Jayatilaka, and M. A. Spackman, "Towards quantitative analysis of intermolecular interactions with Hirshfeld surfaces," *Chem. Commun.*, no. 37, pp. 3814-3816, 2007. doi: 10.1039/B704980C

[64] C. S. Brown, M. S. Lee, D. W. Leung, T. Wang, W. Xu, P. Luthra, *et al*., "In silico derived small molecules bind the filovirus VP35 protein and inhibit its polymerase cofactor activity," *J. Mol. Biol.*, vol. 426, no. 10, pp. 2045-2058, 2014. doi: 10.1016/j.jmb.2014.01.010

[65] A. P. Garner, J. M. Gozgit, R. Anjum, S. Vodala, A. Schrock, T. Zhou, *et al*., "Ponatinib inhibits polyclonal drug-resistant KIT oncoproteins and shows therapeutic potential in heavily pretreated gastrointestinal stromal tumor (GIST) patients," *Clin. Cancer Res.*, vol. 20, no. 22, pp. 5745-5755, 2014. doi: 10.1158/1078-0432.CCR-14-1397

[66] C. Bartolucci, E. Perola, C. Pilger, G. Fels, and D. Lamba, "Three-dimensional structure of a complex of galanthamine (Nivalin) with acetylcholinesterase from Torpedo californica: Implications for the design of new anti-Alzheimer drugs," *Proteins Struct. Funct. Bioinform.*, vol. 42, no. 2, pp. 182-191, 2001. doi: 10.1002/1097-0134(20010201)42:2<182:AID-PROT1012>3.0.CO;2-7

[67] Trott and A. J. Olson, "AutoDock Vina: Improving the speed and accuracy of docking with a new scoring function, efficient optimization, and multithreading," *J. Comput. Chem.*, vol. 31, no. 2, pp. 455-461, 2010. doi: 10.1002/jcc.21334

[68] Dassault Systèmes BIOVIA, *Discovery Studio Visualizer*, Version 2017, San Diego, CA, USA, 2017.

[69] A. Daina, O. Michielin, and V. Zoete, "SwissADME: A free web tool to evaluate pharmacokinetics, drug-likeness, and medicinal chemistry friendliness of small molecules," *Sci. Rep.*, vol. 7, p. 42717, 2017. doi: 10.1038/srep42717

[70] M. H. Islam and M. A. Hannan, "Schiff bases: Contemporary synthesis, properties, and applications," IntechOpen, 2024. doi: 10.5772/intechopen.114850

[71] Huang, Z. Zeng, and Q. Huang, "The crystal structure of (*E*)-2-methoxy-6-(((5-methyl-1,3,4-thiadiazol-2-yl)imino)methyl)phenol, C11H11N3O2S," *Zeitschrift für Kristallographie - New Crystal Structures*, vol. 239, no. 1, pp. 51-52, 2024. doi: 10.1515/ncrs-2023-0135

[72] A. Özek Yıldırım, M. Gülsu, and Ç. Albayrak Kaştaş, "Synthesis, crystal structure, and computational studies of a new Schiff base compound: (E)-4-bromo-2-ethoxy-6-{[(2-methoxyphenyl)imino]methyl}phenol," *Structure Reports*, vol. 74, no. 3, pp. 319-322, 2018. doi: 10.1107/S2056989018002062

[73] H. H. Tang, L. Zhang, L. L. Zeng, X. M. Fang, L. R. Lin, and H. Zhang, "A pair of Schiff base enantiomers studied by absorption, fluorescence, electronic and vibrational circular dichroism spectroscopies and density functional theory calculation," *RSC Adv.*, vol. 5, no. 46, pp. 36813-36819, 2015. doi: 10.1039/C5RA04885A

[74] Fukui, "Role of frontier orbitals in chemical reactions," *Science*, vol. 218, no. 4574, pp. 747-754, 1982. doi: 10.1126/science.218.4574.747

[75] G. Parr and W. Yang, *Density-functional theory of atoms and molecules*. Oxford University Press, 1989.

[76] P. K. Chattaraj, U. Sarkar, and D. R. Roy, "Electrophilicity index," *Chem. Rev.*, vol. 106, no. 6, pp. 2065-2091, 2006. doi: 10.1021/cr040109f

[77] Y. Zhang, G. Lu, J. Li, Y. Wang, and G. Yang, "Study on the electronic and optical properties of organic dye sensitizers using DFT and TD-DFT," *J. Mol. Struct.*, vol. 1015, pp. 77-84, 2012. doi: 10.1016/j.molstruc.2011.12.048

[78] A. P. de Silva, H. Q. N. Gunaratne, and C. P. McCoy, "A molecular photoionic AND gate based on fluorescent signaling," *Nature*, vol. 364, no. 6434, pp. 42-44, 1993. doi: 10.1038/364042a0

[79] P. Politzer and J. S. Murray, "The fundamental nature and role of the electrostatic potential in atoms and molecules," *Theor. Chem. Acc.*, vol. 108, pp. 134-142, 2002. doi: 10.1007/s00214-002-0363-9

[80] C. H. Suresh, V. Krishnakumar, G. Sudhakar, and R. Aravind, "Molecular electrostatic potential analysis: A powerful tool to predict chemical reactivity and non-covalent interactions in molecules," *J. Mol. Struct.*, vol. 1250, p. 131705, 2022. doi: 10.1016/j.molstruc.2021.131705

[81] A. D. MacKerell, "Empirical force fields for biological macromolecules: Overview and issues," *J. Comput. Chem.*, vol. 25, no. 13, pp. 1584-1604, 2004. doi: 10.1002/jcc.20082

[82] P. Bouanich and A. Predoi-Cross, "Theoretical calculations for line-broadening and pressure-shifting in the fundamental and first two overtone bands of CO-H_2," *J. Mol. Struct.*, vol. 742, no. 1-3, pp. 183-190, 2005. doi: 10.1016/j.molstruc.2005.01.004

[83] A. Bosshard, M. Bösch, I. Liakatas, M. Jäger, and P. Günter, "Second-order nonlinear optical organic materials: Recent developments," in *Nonlinear Optical Effects and Materials*, Springer, 2000, pp. 163-299.

[84] P. P. Kuzhir et al., "Onion-like carbon based polymer composite films in microwaves," *Solid State Sci.*, vol. 11, no. 10, pp. 1762-1767, 2009. doi: 10.1016/j.solidstatesciences.2008.12.003

[85] A. E. Reed, L. A. Curtiss, and F. Weinhold, "Intermolecular interactions from a natural bond orbital, donor-acceptor viewpoint," *Chem. Rev.*, vol. 88, no. 6, pp. 899-926, 1988. doi: 10.1021/cr00088a005

[86] F. Jensen, *Introduction to Computational Chemistry*, 3rd ed. John Wiley & Sons, 2017.

[87] C. Ravikumar, I. H. Joe, and V. S. Jayakumar, "Charge transfer interactions and nonlinear optical properties of push-pull chromophore benzaldehyde phenylhydrazone: A vibrational approach," *Chem. Phys. Lett.*, vol. 460, no. 4-6, pp. 552-558, 2008. doi: 10.1016/j.cplett.2008.06.042

[88] F. Weinhold, Discovering Chemistry with Natural Bond Orbitals. John Wiley & Sons, 2012.

[89] S. Mulliken, "Criteria for the construction of good self-consistent-field molecular orbital wave functions, and the significance of LCAO-MO population analysis," *J. Chem. Phys.*, vol. 36, no. 12, pp. 3428-3439, 1962. doi: 10.1063/1.1732745

[90] Ş. Çakmak, B. Koşar Kırca, A. Veyisoğlu, H. Yakan, C. C. Ersanlı, ve H. Kütük, "Experimental and theoretical investigations on a furan-2-carboxamide-bearing thiazole: Synthesis, molecular characterization by IR/NMR/XRD, electronic characterization by DFT, Hirshfeld surface analysis and biological activity," *Crystal Structure Communications*, vol. 78, no. 3, pp. 201–211, 2022. doi: 10.1107/S2053229622001776

[91] Shyamapada, M. Christoph, ve S. Mitra, "Acta Crystallographica Section B: Structural Science, Crystal Engineering and Materials," *Acta Crystallogr. Sect. B*, vol. 63, pp. 129-137, 2016. doi: 10.1107/S0108768109008780

[92] Başak, Antitumor and anticarcinogenic activity of some Schiff base molecules studied by molecular docking, Master's Thesis, Sinop University, Graduate Education Institute, 2023.

[93] Anwar, P. Kumar, ve A. U. Khan, "Modern tools and techniques in computer-aided drug design," M. S. Koumar, Ed., *Molecular docking for computer-aided drug design*, Academic Press, pp. 1-22, 2021. doi: 10.1016/B978-0-12-823549-6.00001-2

[94] X.-Y. Meng, H.-X. Zhang, M. Mezei, ve M. Cui, "Molecular docking: A powerful approach for structure-based drug discovery," *Curr. Comput.-Aided Drug Des.*, 2012. doi: 10.2174/157340911795677602

[95] G. Ferreira, R. N. dos Santos, G. Oliva, ve A. D. Andricopulo, "Molecular docking and structure-based drug design strategies," *Molecules*, vol. 20, no. 7, pp. 13384-13421, 2015. doi: 10.3390/molecules200713384

[96] Pinzi ve G. Rastelli, "Molecular docking: Shifting paradigms in drug discovery," *Int. J. Mol. Sci.*, vol. 20, no. 18, p. 4331, 2019. doi: 10.3390/ijms20184331

[97] B. Banaganapalli, F. A. Morad, M. Khan, C. S. Kumar, R. Elango, Z. Awan, ve N. A. Shaik, "Molecular docking," in *Essentials of Bioinformatics, Volume I: Understanding Bioinformatics: Genes to Proteins*, pp. 335-353, 2019.

[98] A. J. Owoloye, F. C. Ligali, O. A. Enejoh, A. Z. Musa, O. Aina, E. T. Idowu, ve K. M. Oyebola, "Molecular docking, simulation, and binding free energy analysis of small molecules as Pf HT1 inhibitors," *PloS One*, vol. 17, no. 8, p. e0268269, 2022. doi: 10.1371/journal.pone.0268269

[99] D. F. McGinnity, J. Collington, R. P. Austin, ve R. J. Riley, "Evaluation of human pharmacokinetics, therapeutic dose and exposure predictions using marketed oral drugs," *Curr. Drug Metab.*, vol. 8, no. 5, pp. 463-479, 2007. doi: 10.2174/138920007782151895

[100] P. M. Gleeson, A. Hersey, ve S. Hannongbua, "In silico ADME models: A general assessment of their utility in drug discovery applications," *Curr. Top. Med. Chem.*, vol. 11, no. 4, pp. 358–381, 2011. doi: 10.2174/156802611794863691

[101] S. G. Summerfield, A. J. Stevens, L. Cutler, M. del Carmen Osuna, B. Hammond, S. P. Tang, A. Hersey, D. J. Spalding, ve P. Jeffrey, "Improving the in vitro prediction of in vivo central nervous system penetration: Integrating permeability, P-glycoprotein efflux, and free fractions in blood and brain," *J. Pharmacol. Exp. Ther.*, vol. 316, no. 3, pp. 1282-1290, 2006. doi: 10.1124/jpet.105.092916

[102] P. F. Hollenberg, U. M. Kent, ve N. N. Bumpus, "Mechanism-based inactivation of human cytochromes P450s: Experimental characterization, reactive intermediates, and clinical implications," *Chem. Res. Toxicol.*, vol. 21, no. 1, pp. 189-205, 2008. doi: 10.1021/tx700282x

[103] P. Gleeson, "Generation of a set of simple, interpretable ADMET rules of thumb," *J. Med. Chem.*, vol. 51, no. 4, pp. 817-834, 2008. doi: 10.1021/jm701198b

[104] J. D. Hughes et al., "Physiochemical drug properties associated with in vivo toxicological outcomes," *Bioorg. Med. Chem. Lett.*, vol. 18, pp. 4872-4875, 2008. doi: 10.1016/j.bmcl.2008.07.071

[105] J. A. Arnott ve S. L. Planey, "The influence of lipophilicity in drug discovery and design," *Expert Opin. Drug Discov.*, vol. 7, no. 10, pp. 863-875, 2012. doi: 10.1517/17460441.2012.714363

[106] H. van De Waterbeemd, D. A. Smith, K. Beaumont, ve D. K. Walker, "Property-based design: optimization of drug absorption and pharmacokinetics," *J. Med. Chem.*, vol. 44, no. 9, pp. 1313-1333, 2001. doi: 10.1021/jm000407e

[107] C. A. Lipinski, F. Lombardo, B. W. Dominy, ve P. J. Feeney, "Experimental and computational approaches to estimate solubility and permeability in drug discovery and development settings," *Adv. Drug Deliv. Rev.*, vol. 46, no. 1-3, pp. 3-26, 2001. doi: 10.1016/S0169-409X(00)00129-0

[108] L. Di, E. H. Kerns, ve G. T. Carter, "Drug-like property concepts in pharmaceutical design," *Curr. Pharm. Des.*, vol. 15, no. 19, pp. 2184-2194, 2009. doi: 10.2174/138161209788682479